VHDL-AMS modeling of adaptive electrostatic harvester of vibration energy with dual-output DC-DC converter

Andrii Dudka
Paris-VI university, LIP6 laboratory
b.c. 167, 4, place Jussieu
75252 Paris, France
andrii.dudka@asim.lip6.fr

Dimitri Galayko
Paris-VI university, LIP6 laboratory
b.c. 167, 4, place Jussieu
75252 Paris, France
dimitri.galayko@lip6.fr

Philippe Basset
Université Paris-Est, ESYCOM, EA 2552, ESIEE
2, Boulevard B. Pascal, BP 99
93162 Noisy le Grand, France
p.basset@esiee.fr

ABSTRACT

This paper presents a functional design and modeling of smart conditioning circuit of a vibrational energy harvester based on electrostatic transducer. Two original features are added to the basic configuration previously published (whose model we presented on BMAS2007 conference). Firstly, we developed an auto-calibration block which allows the new harvester to adapt dynamically to the varying environment parameters (e.g., amplitude of external vibrations). Secondly, we propose an original schematic configuration based on dual output DC-DC converter, which implements a smart power interface with the load, allowing the harvester to manage a possibly variable load and adapt to different situations (e.g. unsufficient generated power level, load too large, etc.). The scheme of the power interface re-uses the coil existing in the basic harvester configuration. The new harvester architecture contains "software" blocks which can be programmed to implement different power-management and auto-calibration strategies. We describe one possible algorithm of the whole architecture operation, and present the corresponding modeling results. The system is implemented as a mixed VHDL-AMS/ELDO model.

Keywords

Energy harvesting, VHDL-AMS, adaptive switch, dc-dc convertor, MEMS, power management

1. INTRODUCTION

Generation of electricity from available ambiant energies is one of the most promising techniques of supplying low-power autonomous microsystems. Our research is focused on conversion of the energy from environment mechanical vibrations into electricity. Such supply generators can be used in microsystems embedded in moving objects (aircraft, cars, industrial tools, human body etc.), or in vibrating mechanical structures (bridges, ladders, etc.). Particularly, we are interested in harvesters using electrostatic (capacitive) transducers for electromechanical energy conversion. Harvesting the vibration energy with capacitive transducers requires complex conditioning electronics for managing the charge-discharge cycle of electromechanical energy conversion and for interfacing the transducer with the load. The conditioning electronics must take into account varying environment parameters (typically, frequency and amplitude of external vibrations): this requires a "smart" power management and adaptive control of the system operation. However, few studies have adressed these points, and the underlying theory is not mature yet [1]. Our work concerns the power management in environment-adaptive conditioning circuit for electrostatic vibration energy harvester. Here we present original architecture and algorithm of smart energy harvesting system based on capacitive transducer, and describe its mixed VHDL-AMS/ELDO model.

This study continues the work presented in [2], which concerned modeling of harvester with architecture initially proposed in [3]. This basic configuration demonstrated well the physical principle of the energy harvesting with the use of capacitive transducer, but the issues related to adaptation to environment conditions and with power management were not adressed. The new harvester architecture and its model which we present here are based on the model which was published in [2], with two new features. Firstly, we designed and modeled a calibration block which adapts "in real time" the operation parameter of the coniditioning circuit to the external vibrations. Secondly, we improved the basic architecture [3] by adding a second output to the existing flyback circuit DC-DC convertor. This allows a generation of low DC voltage for the load without using an additional DC-DC convertor, which would require an additional inductor. We present the global VHDL-AMS/ELDO model of the system with the simulation results.

2. BASIC ARCHITECTURE AND MOTIVATIONS FOR IMPROVEMENTS

The basic architecture of the harvester is composed of a charge pump, of a flyback circuit and of a switch SW controlling the flyback circuit (fig. 1). The capacitors are initially pre-charged with some external energy sources. The role of the charge pump circuit is to transfer electrical charges from a large capacitor C_{res} to a smaller capacitor C_{store} making use of variation of the transducer capacitance C_{var}. The energy for this charge pumping comes from the mechanical domain, and during pumping, the harvested en-

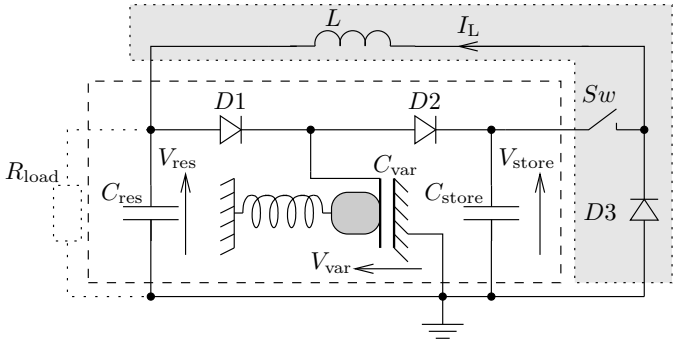

Figure 1: Conditioning circuit of vibration energy harvester.

ergy is stored in the capacitive network composed of C_{res} and C_{store} connected in series. Quantitatively, the energy is represented by C_{res} and C_{store} voltage difference, but since $C_{res} >> C_{store}$, during pumping V_{res} remains nearly constant, and only the V_{store} evolution represents the accumulation of energy.

Thin lines in fig. 2a demonstrate the evolution of V_{store} and of the generated power during the charge pump operation. After some time, V_{store} saturates and the harvested power decreases. To continue the energy harvesting, it is necessary to decrease the voltage difference between C_{store} and C_{res} without loosing the harvested energy. It is performed by a flyback circuit, which operates as a Buck DC-DC converter, transfering charges from C_{store} to C_{res} using the inductor as an energy buffer. The flyback operation is controlled by the switch Sw.

From the thin curve in fig. 2b it is seen that there is some time interval where the generated power is maximal. This corresponds to some V_1 and V_2 limit values of V_{store} (fig.2a). Hence, to continuosly harvest the energy, V_{store} should remain in this range, varying periodically (cf. bold line plots in the fig. 2). For this, when V_{store} reaches V_2, Sw should switch on, the Buck DC-DC converter transfers the charges and the energy from C_{store} to C_{res}. Sw should turn off when V_{store} is reduced to V_1. As we showed in [2], automatic generation of the switching events is possible if the switch control block senses the voltage V_{store} and V_{res} and detects the crossing of the threshold values V_1 and V_2 by V_{store}. Theoretical investigation provides us with following semi-empirical formula for V_1 and V_2 calculation [4]:

$$\begin{aligned} V_1 &= V_{res} + 0.1 \cdot (V_{store\,max} - V_{res}), \\ V_2 &= V_{res} + 0.6 \cdot (V_{store\,max} - V_{res}). \end{aligned} \quad (1)$$

Here $V_{store\,max}$ is the saturation voltage of the charge pump (fig. 2) given by [3]:

$$V_{store\,max} = V_{res} \cdot C_{max}/C_{min}, \quad (2)$$

where C_{max} and C_{min} are the maximal and minimal values of the transducer capacitance.

This architecture, whose VHDL-AMS/ELDO model is presented in [2], has two fundamental drawbacks. Firstly, from eq. (2), $V_{store\,max}$ depends on C_{max} and C_{min} which depends on the resonator vibration amplitude. The latter, in

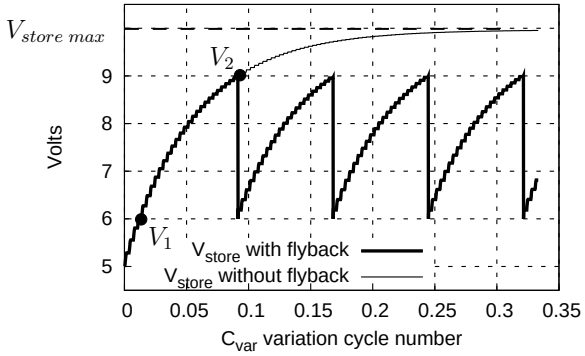

a)

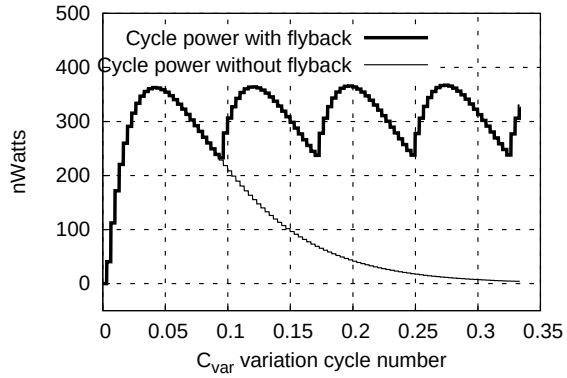

b)

Figure 2: Operation of the harvester with basic architecture: a) V_{store} evolution; b) Power evolution.

turn, depends on the parameter of the external vibrations, unknown *a priori* and which can not be measured. Secondly, theoretical investigations presented in [4] highlight that optimal power yield requires high voltage level on C_{res} (tens of volts), whereas usually, the load is supplied by few volts voltages. To generate a low voltage, a DC-DC convertor is needed, which would consist in an additional energy convertion stage, and would require an additional inductor. These drawbacks are adressed by the improvements which we present in the next two sections.

3. AUTO-CALIBRATION OF THE SYSTEM

As presented in sect. 2, the threshold voltages V_1 and V_2 are optimized for particular parameters of external vibrations. To update V_1 and V_2 when the external vibration frequency and amplitude change, the current value of the parameter $V_{store\,max}$ should be known (eq. (1)). $V_{store\,max}$ can not be measured directly, since during the energy harvesting cycle V_{store} never reaches the saturation (fig. 2a). Hence, $V_{store\,max}$ can only be measured in an *ad-hoc* calibration cycle, which should be repeated periodically so to account for the variation of external vibration parameters. Since such measurements consume energy, a compromise should be found between the frequency (and hence, precision) of V_1 and V_2 update and the energy consumed by the calibration. The proposed technique of calibration can be summarized as follows. To measure $V_{store\,max}$, we desactivate the flyback circuit and let the charge pump run freely up to the saturation. So, the saturation value of V_{store} can be measured and can be used as $V_{store\,max}$ in V_1 and V_2 calculation.

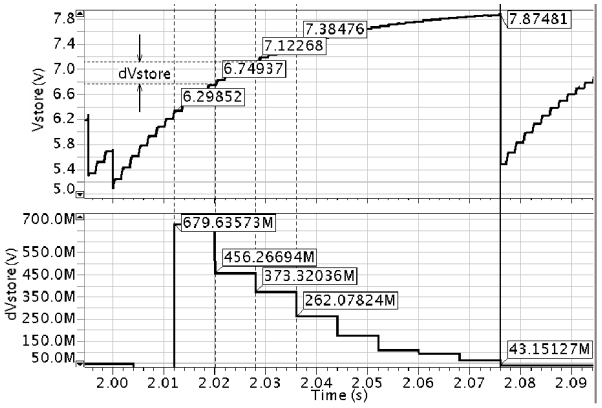

Figure 3: Calibration phase operation.

The algorithm of the calibration cycle is the following. In the begining of each calibration cycle, V_{store} value is reset to V_{res}, to place the charge pump in the inital state (fig. 2a). Then the flyback circuit is desactivated: for this V_2 voltage is temporarily set to a high unreachable value during the whole calibration cycle. To detect the V_{store} saturation, periodic measurements of V_{store} value are done during the calibration cycle. At each measurement, V_{store} is compared with the previously measured value (fig. 3). When the difference ($dVstore$) between two neighboring measured values of V_{store} becomes lower than a predefined value ΔV_{min}, it is concluded that C_{store} voltage is saturated and the last measured value is considered as $V_{store\,max}$. After the $V_{store\,max}$ measurement, V_1 and V_2 are calculated and the calibration cycle ends. Between two calibration cycles, the system operates with updated V_1 and V_2 which are likely to optimise the energy yield.

The presented algorithm of auto-calibration is integrated into the existing VHDL-AMS model of the flyback switch [2]. This new model implements the switch SW as two-terminal electrical component which can be integrated in an ELDO electrical model of the conditioning circuit. The model has two input parameters : V_{store} and V_{res}, which are used by the described algorithm for V_1 and V_2 calculation and for generation of the switching events. The structure of the developed VHDL-AMS model of the new flyback switch is shown in figure 4. It is composed of two functional blocks and uses five processes. The model uses two clocks generated internally: a slow clock (clk) ordering the start of the calibration cycles, and a quick clock (clk_m) ordering the V_{store} measurements.

The calibration block includes four processes. When the signal clk arrives (process 1), V_{store} reset process is activated (process 2). It measures V_{store} and if it is far from V_{res}, V_{store} voltage is reset to V_{res}. After V_{store} is initialized, $V_{store\,max}$ measurement starts in the process 3, and $V_{store\,max}$ is detected as it was explained above. After this, process 4 calculates V_1 and V_2 values: this is the end of the calibration cycle. The calculated V_1 and V_2 values are the input signals of the switching block. In this model, V_1 and V_2 are updated only at the end of the calibration cycle and are kept constant up to the next calibration.

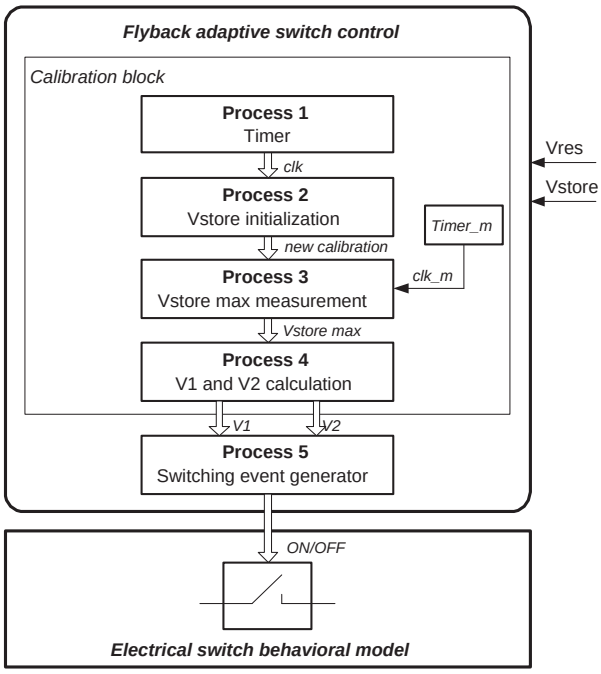

Figure 4: Structure of adaptive flyback switch

The switch control is implemented in the process 5. This process is always active. It detects the V_{store} crossing with V_1, V_2 and generates "on/off" switching events which order the electrical state of the switch. The "electrical switch behavioural model" block is the same as that presented in [2].

The $V_{store\,max}$ measurement (process 3) represents the most important functionality of the calibration block, for this reason we give here the listing of its VHDL-AMS code.

```
P3: PROCESS( new_calibration ,clk_m)
--v_1, v_2 - intermediate Vstore values:
variable v_1: real:=5.0;
variable v_2: real:=5.1;
variable dv: real:=0.0;--dVstore
variable dv_last: real:=0.0;--last dVstore
variable dv_min: real:=5.0e-2; --minimal dVstore
-- parity of the measurement cycle number:
variable par: boolean:=true;
--counter of the clock event:
variable count:real:=0.0;
--internal clock period:
constant clkp:time:=8.0 ms;
BEGIN
 if new_calibration then
--begin calibration: Vstore max measurement starts
   end_calibration<=false;
--dv mesurement
   if clk_m'event and clk_m='1' then
     dv_last:=dv;
     if par then
       v_1:=v_store;
       if v_2>0.0 then
         dv:=v_1-v_2;
       end if;
     else
       v_2:=v_store;
       if v_1>0.0 then
         dv:=v_2-v_1;
       end if;
     end if;
```

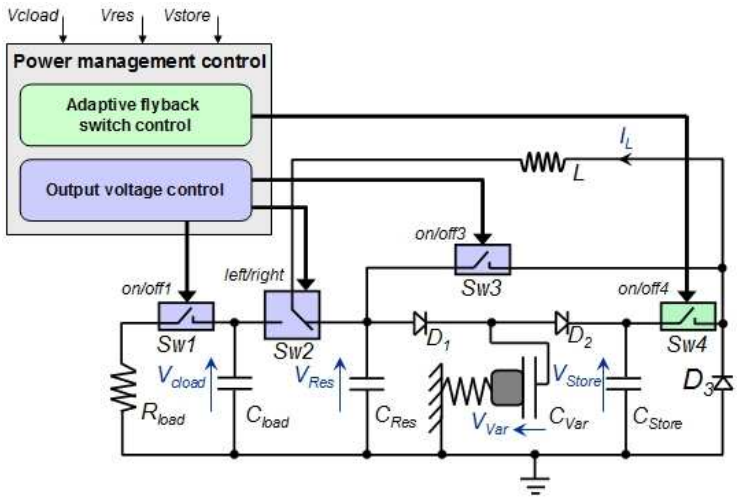

Figure 5: Conditioning circuit of energy harvester with power management control

```
    par:=not par;
--dv minimal value detection:
--active only after 3 measurements of Vstore
    if dv<dv_min and count>3.0 then
       v_store_max<=v_store;
          end_calibration<=true;
       count:=0.0;
    end if;
    count:=count+1.0;
  end if;
  clk_m<=not clk_m after clkp/2;
end if;
END PROCESS P3;
```

4. POWER MANAGEMENT OF THE HARVESTED ENERGY

4.1 Hardware architecture

As mentionned in sec. 2, the optimal energy yield requires high V_{res} voltages (tens of volts), which cames in contradiction with the low-voltage supply requirement for the load. The solution we propose is to add a large capacitor C_{load} to the basic configuration of fig. 1. This capacitor must be charged to a low voltage and is destinated to store the energy immediately available for the load (fig. 5). To charge this capacitor with the energy available in the high-voltage capacitor C_{res}, a DC-DC converter is needed. However, the basic architecture already contains a Buck DC-DC converter implemented by the inductor and the diode $D3$ and used by the flyback circuit. Its role is to transfer the energy from the high voltage C_{store} capacitor to the lower voltage C_{res} capacitor. This DC-DC convertor can be directly used to charge C_{load}. This is done by introducing a switch SW_2 which allows the inductor to discharge on one of two capacitors. The idea is to allow the flyback circuit to return the energy not only to C_{res} capacitor, but alternatively to C_{res} or C_{load} capacitors.

Apart the possibility of generating a low voltage suitable for the load supply, this configuration allows to control the voltage on C_{res}. Indeed, as the theory shows [4], for each external vibration parameter set there is an optimal value of V_{res}. If, for some reasons, V_{res} is higher than this optimal voltage, the proposed dual-output DC-DC converter can just discharge C_{store} on C_{load} during several cycles by keeping the switch SW_2 in the position "left". This will slowly reduce the charges on C_{res}, since its charges consumed by the charge pump operation will not be compensated by the flyback anymore.

However, the following critical situation is possible. If the external vibration parameters change so that the optimal value of C_{res} voltage needs to be substatially reduced, the presented above dual-output dc-dc converter may not help. Indeed, since C_{res} value is too high, the charge pump may not be able to operate (this issue has been highlighted by theoretical studies [4]). In this context C_{res} voltage can't be reduced without losses. To escape from this situation, we propose to add an additional switch SW_3 which allows to connect C_{res} to the input of the DC-DC converter, and C_{load} to the output. Thus, if the voltage V_{res} has to be quickly reduced, two switches are activated: SW_2 (position left) and SW_3 (on). The capacitor C_{res} discharges on C_{load}, and the control block cut off the switch SW_3 when C_{res} come down to the wanted value.

The switch SW_1 is added to interface the load with the harvester. It is an important part of the power management infrastructure: it allows, for example, to disconnect the load from the generator if the harvested power is low, hence avoiding discharge of the capacitors C_{load} and C_{res}. The switches SW_1-SW_3 are supposed to be controlled by some smart electronics which sense the voltages V_{cload} and V_{res}, and which, depending on the application and the nature of the load, implements some optimal power measurement strategy.

4.2 Model of harvester with power management

The model of the improved architecture of harvester with power management block (fig. 5) is implemented in the same way as the basic model (fig. 1) [2]: the Eldo netlist of the schematic of fig. 5 includes electric components (diodes, ca-

pacitors) and VHDL-AMS electical models of resonator and four switches $SW_1 - SW_4$. Switches SW_1, SW_3 and SW_4 are implemented as instances of the block "electrical switch behavioural model" in fig. 4. The double switch $SW2$ is implemented in a similar way. The states of the switches are ordered by the corresponding *on/off*$_i$ and *left/right* (for SW_2) signals generated by their control blocks. For example, the flyback adaptive switch is implemented with two blocks shown in fig. 4: the physical switch SW_4 and the "adaptive flyback switch control" block. The latter generates switching events for the former, after processing V_{res} and V_{store} quantities with the algorithm described in sec. 3. In the same way, the "power management control block" receives at the input the voltage of V_{res} and V_{cload} and, depending on the power management strategy for which it is programmed, it generates the ordering events *on/off*$_i$ for the switches SW_1 and SW_3 and *left/right* for SW_2.

The development of the algorithm of the "power management control" block operation is the subject of ongoing work. However, to test our model, we implemented a very simple algorithm consisting in following. The goal is to maintain V_{res} and V_{cload} in fixed limits (V_{R1}, V_{R2}) and (V_{L1}, V_{L2}) respectively. When V_{res} reaches the upper limit V_{R2}, SW_3 becomes on and SW_2 connects L to C_{load} (position left). Thus, C_{res} decharges quickly on C_{load} through L. The switch SW_3 becomes off when V_{res} reduces to V_{R1}. The switch SW_2 goes to position "right" after L discharges completely on C_{load}. After that, the conditioning circuit operates in the normal way until V_{res} becomes over V_{R2} again. Independently of this, the level of V_{cload} is controlled. When V_{load} reaches V_{L2}, the switch SW_1 connects the load resistance to C_{load}, and C_{load} discharges on the load, loosing its energy and hence reducing its voltage. When V_{cload} reduces to V_{L1}, the switch SW_1 becomes off. This algorithm is appropriate in the case, when the load consumes more power than the harvester is able to produce. Hence, the load can only be supplyed by time bursts during which the energy is injected in the load. For example, this operation can be used to rechage an accumulator. However, more complex algorithms can be developped, depending on the specific application.

5. MODELING RESULTS

To validate our study, two modeling experiments were done. The goal of the first one is the comparison of operation of the harvester, which uses the flyback calibration with the basic configuration in which $V_{store\,max}$ is pre-calculated under hypothesis of constant and known parameters of external vibration [2]. Both configurations are identical apart the flyback switch models (with and without calibration), and are modeled in the same context of variable acceleration amplitude of external vibrations. Both configurations don't include nor output voltage control, neither load resistor (fig. 1). The calbiration is done after each 1 s (*clk* period), and *clk_m* clock has a period of 8 ms. The goal of the second expriment is to test the output voltage control block described in sec. 4. This experiment was modeled with constant parameters of external vibrations. For the simulation we used a load resistor of 2 MΩ. The goal of the output voltage control block is to maintain V_{res} within the range (19.5V, 20.5V) and V_{load} in the range (3.2V, 3.6V). Both experiments were run with external vibrations frequency of 298 Hz and used a transducer model with C_{var} variation

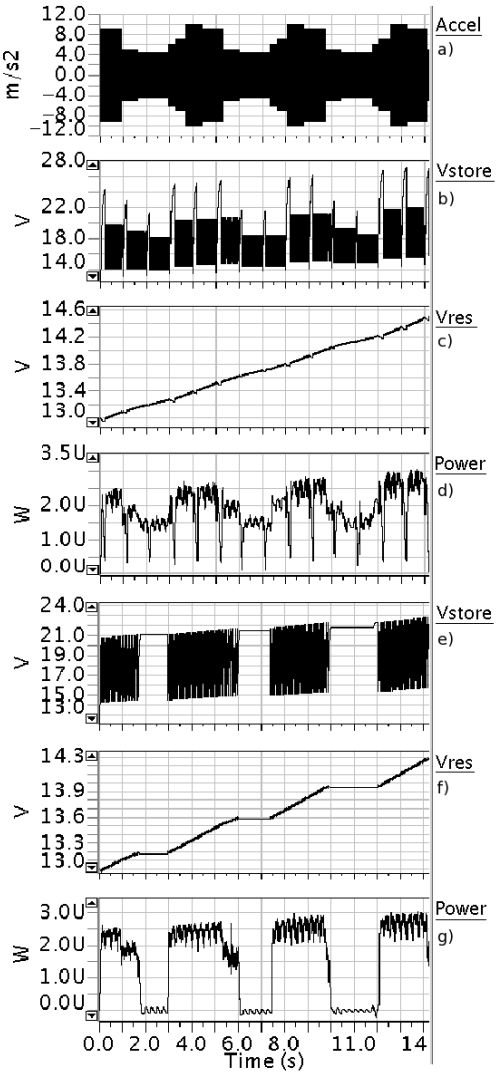

Figure 6: Simulation results of two harvester models: a) acceleration of external vibrations; b),c),d) - behaviour of system with adaptive flyback switch; e),f),g) - behaviour of basic architecture.

between 100 pF and 200 pF. The initial value for C_{res} and C_{store} capacitors was 13 V.

Figure 6 presents the simulation results for the first experiment. The upper plot shows the acceleration of the external vibrations, with amplitude changing over time from 4.5 to 10 ms^{-2}. In the same figure, we present the evolution of characteristic quantities in the two tested models. The plots b),c),d) demonstrate V_{store}, V_{res} and generated power evolution curves respectively for the auto-calibrated system. The plots e),f),g) represent the evolution of the same parameters for the system with the non-adaptive switch. Comparing results of these two simulations, some interesting observations can be done. When the acceleration amplitude of the external vibrations decreases, the system with the non-adaptive switch doesn't harvest energy. It occurs because due to the lower mechanical force, the amplitude of resonator vibration reduces, and C_{var} variation amplitude reduces as well, mod-

ifying C_{max} and C_{min} capacitances so that new $V_{store\,max}$ value (eq. (2)) is less than the V_2 limit value, and flyback can not be activated. In this way, the charge pump is saturated, no energy is harvested and V_{res} voltage remains constant. However, with the use of the auto-calibrated flyback switch (sec. 3), one can observe that the conditioning circuit adapts to the variable amplitude of acceleration and continues the energy harvesting. For example, when the vibration amplitude becomes low, V_1 and V_2 values decrease so to ensure the energy harvesting under those conditions. And inversely, when the acceleration amplitude increases, V_1 and V_2 values become also greater so to provide the system with the maximum possible power of harvested energy. The average power generated by the system with auto-calibration is nearly twice larger than in the case of the basic architecture.

The plots in fig. 7 demonstrate the modeling results of the conditioning circuit presented in the fig. 5. On this plot, one can observe the establishing of the mode of sustainable energy harvesting. The system starts from the state corresponding to zero energy of C_{load} and to 13 V of C_{res} pre-charge. The plots highlight three phase of operation. The first phase continues up to 45 seconds, and corresponds to the accumulation of internal energy of the harvester. Indeed, initially V_{res} is below the wanted range (19.5,20.5 V), hence, during the first phase, all harvested energy is accumulated by C_{res} so to increase its voltage. When V_{res} reaches V_{R2}=20.5 V, the extra energy of V_{res} begins to be transfered toward C_{load}. This transfer is very quick comparing to the average rate of V_{res} evolution, and immediately after this, V_{res} equalizes to V_{R1}. Looking at the V_{cload} evolution, one can observe that between 45 and 85 seconds, the C_{load} accumulates the charges from C_{res}, but doesn't transfer them to the load. This is the second phase: precharge of the energy buffer for the load supply. Indeed, the load can't be supplied with the voltage under V_{L1}, hence, the switch SW_1 is kept off during all the phase 2. Actually, when V_{load} reaches V_{L2}=3.6 V, the switch SW_1 is on and the load is supplied by C_{load}. This is the start of the phase 3 corresponding to sustainable energy generation. Since R_{load} consumes more power that the harvester generates, V_{cload} reduces slowly, and when it reaches V_{L1}, SW_1 disconnects R_{load} from C_{load}, and C_{load} increases its voltage and energy again until $V_{cload} = V_{L2}$.

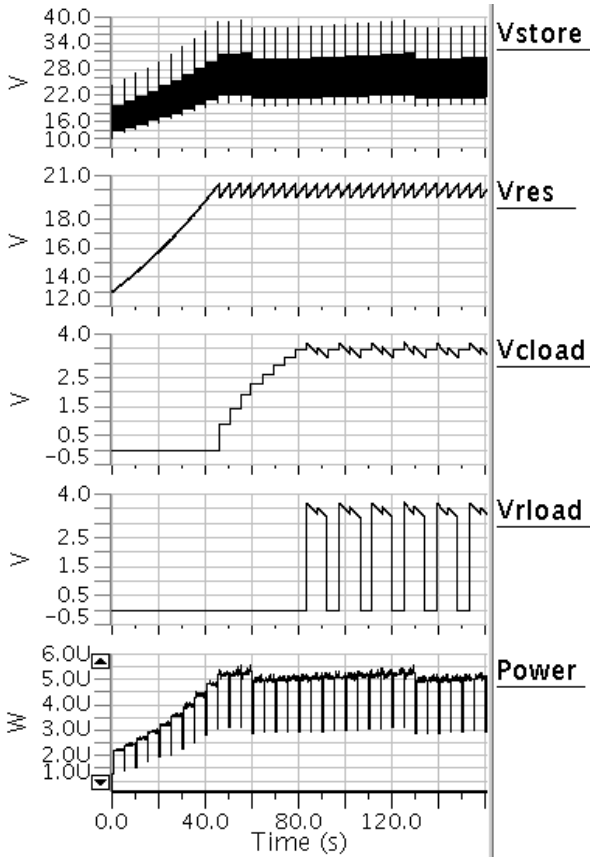

Figure 7: Simulation results of harvester model

6. CONCLUSIONS

This study provides the basic architecture of vibration energy harvester with two new features: the possibility to adapt to the environmental conditions and with smart power interface with the load. To our knowledge, these issues concerning the integration of the harvester into the real environment have never been adressed for the studied basic architecture [3]. The global improved architecture is implemented as VHDL-AMS/ELDO mixed model. The proposed model includes hardware blocks such as switches, resonator and conditioning electronics, and the control blocks which can operate following different algorithms. Hence, this model can be used as the basis for research of the optimal strategy of power management inside the harvester and on the interface between the harvester and the load. Several improvements can be made to the proposed model. Firstly, the switches should be implemented by high-voltage transistors, to adequately model losses and transient phenomena. Secondly, the algorithm of the calibration should take into account the possible measurement losses when detecting the minimal $dVstore$ value, and probably, it should yet be simplified to be more appropriate for low-power hardware implementation. At last, more investigation should be made on dual-output DC-DC converter, its performances and operation algorithm.

7. ACKNOWLEDGEMENTS

This work is funded by the French National Research Agency.

8. REFERENCES

[1] Paul D. Mitcheson, Tim C. Green, Eric M. Yeatman, and Andrew S. Holmes. Architectures for vibration-driven micropower generators. *IEEE JMEMS*, 13(3):429–440, june 2004.

[2] D. Galayko, R. Pizarro, P. Basset, M.A. Paracha, and G. Amendola. AMS modeling of controlled switch for design optimization of capacitive vibration energy harvester. In *IEEE BMAS2007 conference*, pages 115–120, San José, California, USA, september 2007.

[3] B. C. Yen and J. H. Lang. A variable-capacitance vibration-to-electric energy harvester. *IEEE TCAS*, 53(2):288–295, february 2006.

[4] D. Galayko and P. Basset. Mechanical/electrical power-aware impedance matching for design of capacitive vibration energy harvester. In *PowerMEMS2008 workshop, Sendai*, 2008.